Journal of Power Sources 196 (2011) 9985–9988

Contents lists available at ScienceDirect

Journal of Power Sources

journal homepage: www.elsevier.com/locate/jpowsour

Short communication

# Doubling the diffusivity measurement efficiency in solid oxide fuel cells (SOFCs) via a bi-sensor electrochemical cell

Weidong He[a,b,*], Bin Wang[c], Haibo Zhao[d], Yang Jiao[e]

[a] Interdisciplinary Program in Materials Science, Vanderbilt University, Nashville, TN 37235, USA
[b] Vanderbilt Institute of Nanoscale Science and Engineering, Vanderbilt University, Nashville, TN 37235, USA
[c] Department of Physics, Vanderbilt University, Nashville, TN 37235, USA
[d] High-Performance Materials Institute, Florida State University, Tallahassee, FL 32304, USA
[e] Department of Electrical Engineering, Vanderbilt University, Nashville, TN 37235, USA

ARTICLE INFO

*Article history:*
Received 15 June 2011
Received in revised form 8 August 2011
Accepted 9 August 2011
Available online 16 August 2011

*Keywords:*
Diffusivity
Solid oxide fuel cell
Oxygen sensor
Current density
Concentration polarization
Electrode thickness

ABSTRACT

To improve the efficiency of the diffusivity measurement in solid oxide fuel cells (SOFCs), a bi-sensor electrochemical cell is proposed and analyzed. The cell consists of an oxygen pump and two oxygen sensors. This bi-sensor cell doubles the efficiency of binary diffusivity measurements in both porous anodes and cathodes in SOFCs. The design provides an efficient platform to estimate the electrode limiting current density (LCD) and concentration polarization (CP) in SOFCs. Mechanism of measuring the CP with different electrode configurations was discussed in depth. The design was verified by studying the effect of electrode thickness on the CPs at different operating temperatures.



## 1. Introduction

Solid oxide fuel cells (SOFCs) are characterized by their high efficiency, low pollution emission, fuel flexibility and scalable modularity [1–9]. In an electrode-supported SOFC, the maximum current density (CD) is largely limited by the contribution of concentration polarization (CP) at the electrode (anode or cathode) because the thick electrode impedes the transport of both reactant and resultant gases [5,10–14]. The transport of the gas through the electrode is mainly accomplished by diffusion. At a given CD, the concentration polarization of an electrode in a SOFC is a function of the diffusivity of the reactant gas, the partial pressure of the gas, the thickness of the electrode, and the operation temperature [15]. The diffusivity of the gas correlates with the properties of the electrode, such as porosity, pore size, and tortuosity. Thus, it is important to measure the effective diffusivity of the anode or cathode gas under the operating conditions to evaluate the performance of SOFCs [16–18]. Diffusivities and CPs of SOFC electrodes were previously fitted based on multiple voltage-current measurements on the cells. But the validity has remained in debate because the fitted diffusivities and CPs only provide indirect information on the electrodes that are assembled into SOFCs in the measurements [13,19]. Under the operating conditions, the effective diffusivity of $O_2$ and $N_2$ in porous LSM discs has been measured through an electrochemical cell with an oxygen sensor in an out-of-cell fashion [18]. The $H_2$–$H_2O$ effective binary diffusivity measurements in porous Ni and yittria-stabilized zirconia (YSZ) cermet anode using a similar electrochemical cell between 650 and 800 °C were reported recently [16]. Although the two electrochemical cells provide practical out-of-cell diffusivity measurements on electrodes in SOFCs, both cells only have one oxygen sensor at one side of the oxygen pump, leaving the other side unutilized.

In this paper, we proposed and analyzed an electrochemical cell with two oxygen sensors, which allows two anodes or cathodes to be measured simultaneously and, thus, doubles the efficiency of gas-diffusivity measurements in SOFCs. CPs as a function of electrode thickness were evaluated for both anodes and cathodes. We found that the temperature-dependence of concentration polarization varies as a function of the thickness of anodes and cathodes, which, in principle, is helpful for rational design of SOFC to achieve high performance.

* Corresponding author at: Interdisciplinary Program in Materials Science, Vanderbilt University, Nashville, TN 37235, USA. Tel.: +1 6153647338; fax: +1 6153437263.
*E-mail address:* weidong.he@vanderbilt.edu (W. He).

0378-7753/$ – see front matter © 2011 Elsevier B.V. All rights reserved.
doi:10.1016/j.jpowsour.2011.08.048

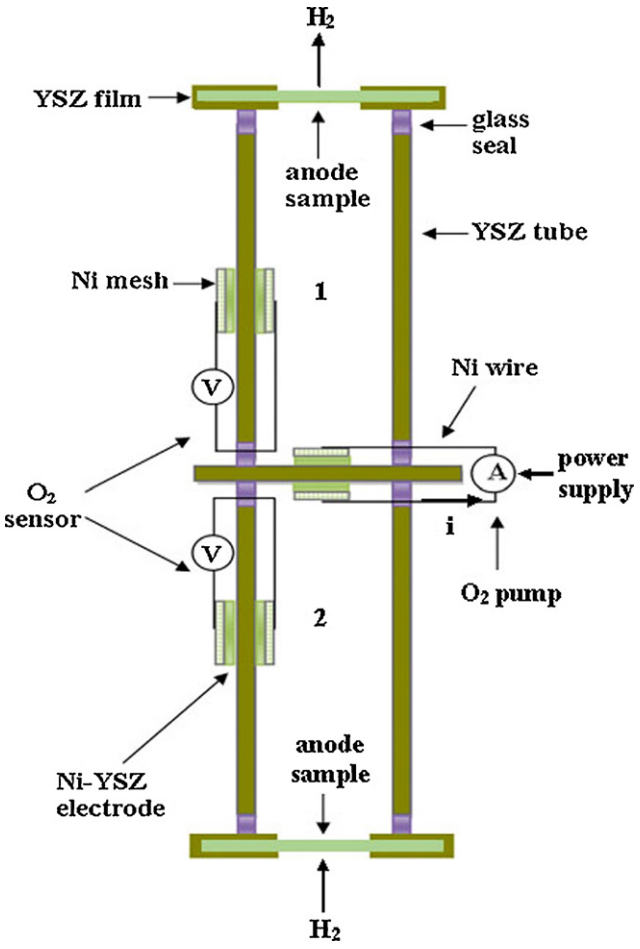


**Fig. 1.** A schematic of the bi-sensor electrochemical cell for the measurement of the effective binary diffusivity in porous anodes in SOFCs. The directions of $H_2$ flow and current provided by the $O_2$ pump are demarcated by arrows.

## 2. Bi-sensor electrochemical cell

The bi-sensor electrochemical cell as proposed is shown in Fig. 1. It consists of two dense YSZ tubes with dimensions similar to those as previously reported, which are connected by a dense YSZ disc with glass seal [16,18]. The inside and outside walls of each tube are installed with an oxygen sensor which consists of Ni-YSZ electrodes, Ni meshes and Ni wires, and a voltage meter. An oxygen pump is installed on both sides of the dense YSZ disc with a current power supply. The tested samples are attached to the two ends of YSZ tubes. The bi-sensor design allows the measurements on oxygen partial pressures in each tube simultaneously and independently. The tested samples can both be two anodes or cathodes. The electrochemical cell can be placed in a tube furnace and measurements can be carried out to measure the gas diffusivities in two anodes or two cathodes. In the case of measuring two anodes, the measurements can be performed above 500 °C with $H_2$–$H_2O$ (97% $H_2$) mixture gas. If the tested samples are both cathodes, the measurements can be conducted with $O_2$–$N_2$ (air).

## 3. Theoretical analysis

The bi-sensor design exhibits versatility on testing different types of electrodes. The theory on measuring CPs for both anodes and cathodes will be derived and discussed.

In a scenario where two porous anode samples are tested, such as Ni-YSZ discs, as $O_2$ is pumped from YSZ tube 1 to YSZ tube 2, the

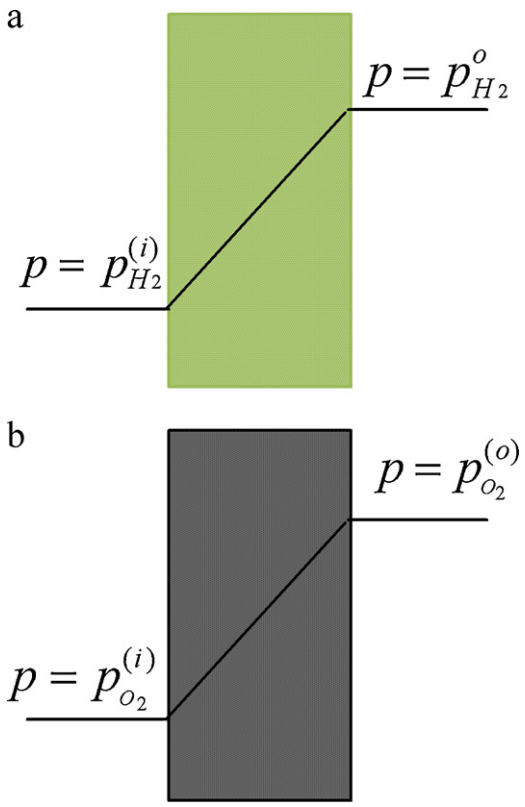


**Fig. 2.** Schematics of porous Ni-YSZ anode sample and LSM cathode sample, along partial pressures of reactant gases.

partial pressure of $H_2$ in tube 1 increases and that of $H_2O$ decreases. As shown in Fig. 2, the two pressure gradients across the pump induce $H_2$ and $H_2O$ fluxes out of and into tube 2 through the porous Ni-YSZ anode sample on tube 2. In the meantime, $H_2$ and $H_2O$ fluxes are generated through the other Ni-YSZ sample on tube 1 in the opposite directions. When the system reaches a steady state, $H_2$ and $H_2O$ fluxes out of and into tube 2 are related to the current density (i) provided by the $O_2$ pump through Eq. (1), where $F$ is the Faraday constant. Since the flux of $H_2$ and that of $H_2O$ are in the opposite directions through one-dimensional diffusion, they can be expressed in Eqs. (2) and (3), where $D^{eff}_{H_2-H_2O}$ is the

$$J_{H_2} = J_{H_2O} = \frac{i}{4F} \tag{1}$$

$$J_{H_2} = \frac{i}{4F} = -D^{eff}_{H_2-H_2O}\nabla n_{H_2} = -\frac{D^{eff}_{H_2-H_2O}}{RT}\frac{dp_{H_2}}{dx} \tag{2}$$

$$J_{H_2O} = -\frac{i}{4F} = -D^{eff}_{H_2-H_2O}\nabla n_{H_2O} = -\frac{D^{eff}_{H_2-H_2O}}{RT}\frac{dp_{H_2O}}{dx} \tag{3}$$

effective binary diffusivity of $H_2$ and $H_2O$, $T$ is the temperature, $R$ is the gas constant, $p_{H_2}$ and $p_{H_2O}$ are $H_2$ and $H_2O$ partial pressures, respectively. Integration over the partial pressures $p_{H_2}$ and $p_{H_2O}$ across the tested sample leads to Eqs. (4) and (5), where $l_a$ is the thickness of the

$$p^{(i)}_{H_2} = p^{o}_{H_2} - \frac{RTl_a}{4FD^{eff}_{H_2-H_2O}}i \tag{4}$$

$$p^{(i)}_{H_2O} = p^{o}_{H_2O} - \frac{RTl_a}{4FD^{eff}_{H_2-H_2O}}i \tag{5}$$

sample, $p^{(i)}_{H_2}$ and $p^{o}_{H_2}$ are the partial pressures of $H_2$, and $p^{(i)}_{H_2O}$ and $p^{o}_{H_2O}$ are the partial pressures of $H_2O$ in and out of tube 2.

The $O_2$ pressure in tube 2 is determined from the Nernst potential read from the $O_2$ sensor on tube 2 through Eq. (6), where $p^{(i)}_{O_2}$ and $p^{o}_{O_2}$ are $O_2$ partial pressures in and out of tube 2. $p^{(i)}_{O_2}$ can be calculated using Eqs. (6)–(8), where, $K_{eq}$ is equilibrium constant. With the value of $p^{(i)}_{O_2}$, $p^{(i)}_{H_2}$ and $p^{(i)}_{H_2O}$ can be obtained using through Eqs. (7) and (8). Therefore, Nernst potentials given by the oxygen sensor directly produces linear plot of $p_{H_2}$ vs. $l_a$ and the slope of the plot enables one to calculate $D^{eff}_{H_2-H_2O}$. $D^{eff}_{H_2-H_2O}$ of the sample on tube 1 can be measured by the routine as recently reported [16].

$$E = \frac{RT}{4F} \ln\left(\frac{p^{(i)}_{O_2}}{p^{o}_{O_2}}\right) \tag{6}$$

$$K_{eq} = \frac{p^2_{H_2O}}{p^2_{H_2} p_{O_2}} \tag{7}$$

$$p_{total} = 1\,\text{atm} \approx p_{H_2} + p_{H_2O} \tag{8}$$

In the case of two cathode samples, calculations based on Nernst potentials of both sensors will lead to the measured values of $D^{eff}_{N_2-O_2}$ using Eq. (9), where $p^{o}_{O_2}$ and $p^{(i)}_{O_2}$ are the $O_2$ pressures in tube 2 before the cell is powered and when the equilibrium of gas pressures is reached during the measurements, respectively. To measure the binary diffusivity of porous cathode samples, cathode gas ($O_2$ + $N_2$) is needed, and cathode materials, such as platinum paste, should be used to make the $O_2$ sensor and the $O_2$ pump [18].

## 4. Discussion

From the above analysis, it is found that the efficiency of binary effective diffusivity measurements is doubled using the as-designed bi-sensor electrochemical cell, and the practical goal is to apply the device to quantitatively evaluate the LCD and CP of electrodes for application consideration. For CP induced by slow mass transport of gas-phase reactants, it is related to LCD by Eq. (10) for anode and Eq. (11) for cathode, where $i_{as}$ and $i_{cs}$, the anode and cathode limiting current density, are approximated by Eqs. (12) and (13), respectively [17,20].

Thin films have been actively studied recently for various applications. Nanostructured thin electrodes are favored in batteries and fuel cells for their advantages over traditional bulk electrodes, such as high power efficiency, long lifetime and high portability [3,4,21–25]. Another favored direction could be using hetero-nanostructures as electrodes where a high porous Si substrate is used to support the SOFCs. The potential advantages for this direction open up practical applicability of these thin film SOFCs. Similar to bulk SOFCs, it is necessary to evaluate the

$$p^{(i)}_{O_2} \approx p^{o}_{O_2} + \frac{RTl_a}{8FD^{eff}_{N_2-O_2}} i \tag{9}$$

$$\eta_{a,conc} = -\frac{RT}{2F} \ln\left(1 - \frac{i}{i_{as}}\right) + \frac{RT}{2F} \ln\left(1 + \frac{p^{o}_{H_2} i}{p^{o}_{H_2O} i_{as}}\right) \tag{10}$$

$$\eta_{a,conc} = -\frac{RT}{4F} \ln\left(1 - \frac{i}{i_{cs}}\right) \tag{11}$$

$$i_{as} \approx \frac{4Fp^{o}_{H_2} D^{eff}_{H_2-H_2O}}{RTl_a} \tag{12}$$

$$i_{cs} \approx \frac{8Fp^{o}_{O_2} D^{eff}_{O_2-N_2}}{RTl_c} \left(\frac{p_t}{p_t - p^{o}_{O_2}}\right) \tag{13}$$

performance of these nanostructured electrodes before their assembly and operation. The bi-sensor device is an effective tool to evaluate the performance of SOFCs with thin electrodes. To demonstrate the correlation between CP and electrode thickness, CP vs. $l_a$ is plotted, as shown in Fig. 3(a). For the plots, the total pressure $p_t$ is fixed at 1 atm at different temperatures and the values of $D^{eff}_{H_2-H_2O}$ at different temperatures are taken from previous report, assuming that the tortuosity and porosity of the tested anode sample is independent on $l_a$ [16].

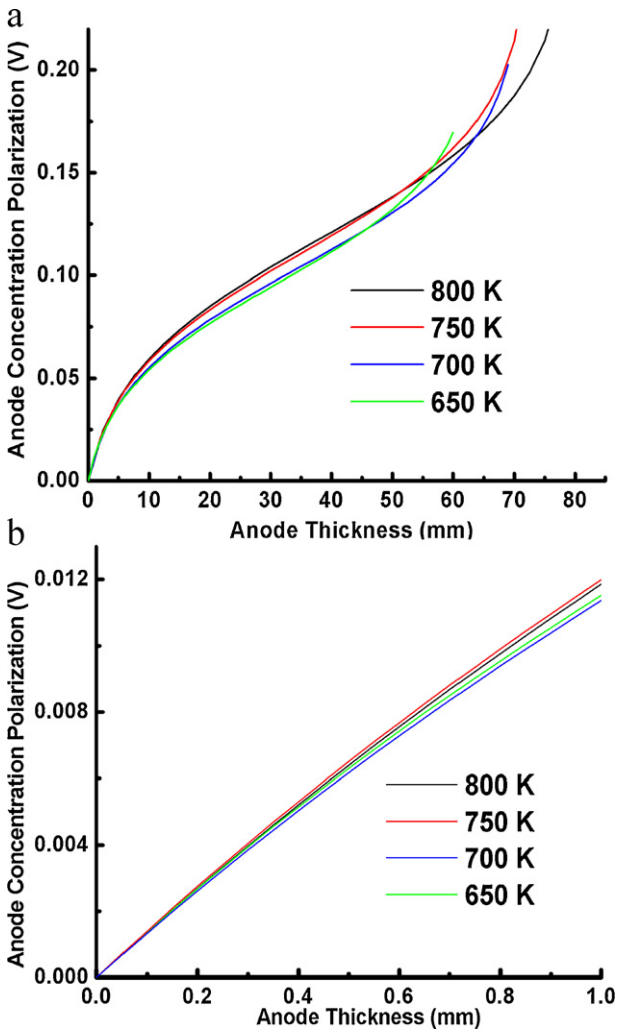


**Fig. 3.** (a) Concentration polarization as a function of anode thickness at different temperatures with a current density of 0.5 A cm$^{-2}$. (b) Enlarged plots of concentration polarization as a function of anode thickness.

A similar plot for cathode measurement is shown in Fig. 4(a). For anode samples, the CPs increases rapidly below the thickness of 10 mm. Above 60 mm, the slope keeps increasing up to infinity. Between the two values, the CPs increase at a relatively small slope of approximately 2.0 mV mm$^{-1}$. The increase of CPs is less sensitive to the thickness from 10 to 60 m, and, thus, increasing the thickness of anodes is advised when the improvement in the mechanical strength and lifetime of SOFCs is desirable. Another interesting feature of the plots is that a greater diffusivity does not necessarily lower CPs. Larger CPs were observed at higher temperatures for anode thickness between 10 mm and 60 mm, e.g. CP loss at 800 °C is the largest, which is contradictory to what is found in Ref. [12] where the anode thickness is out of the range from 0.01 m to 0.06 m. The result is due to the opposite contributions of diffusivity and $T$ to CPs, as shown in Eq. (12) where diffusivity is in the numerator while $T$ is in the denominator. The order of the CP values for different temperatures changes as the thickness of the anode

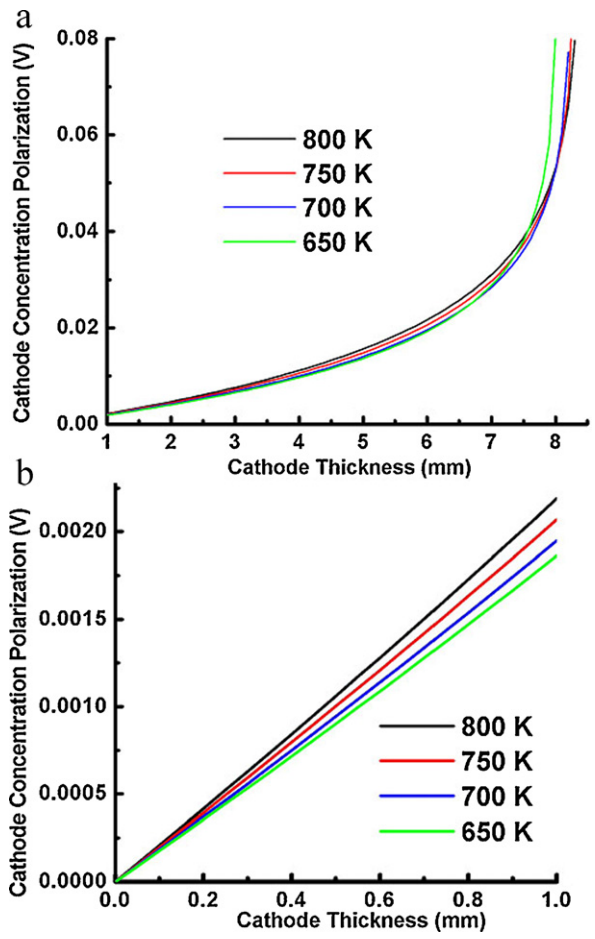


**Fig. 4.** (a) Concentration polarization as a function of cathode thickness at different temperatures with a current density of 0.5 A cm$^{-2}$. (b) Enlarged plots of concentration polarization as a function of cathode thickness.

increases. The phenomenon suggests that it is not always favorable to monotonously increase operation temperature for a SOFC to achieve low CP loss; an appropriate thickness of anodes has to be chosen when determining the best working temperature for a SOFC. Therefore, with the $D^{eff}_{H_2-H_2O}$ and $D^{eff}_{N_2-O_2}$ measured using the proposed bi-sensor cell, the results will provide practical guidance for one to choose the most efficient thickness of anodes as well as the operation temperature of a SOFC.

Compared to anodes, the plots of CPs vs. $l_c$ for cathodes are more simplified. As shown in Fig. 4(a), the order of CP values for the four temperatures only varies once at 8 mm, below which the CP for 800 °C is the largest among the four *T*s at a fixed thickness. Besides, CPs increase more rapidly as the thickness of cathodes increases, with almost vertical slopes above a value of 8 mm, which is almost one order of magnitude smaller than the critical thickness of anodes. The results indicate that it is practical to increase the thickness of cathodes below its critical thickness to improve the lifetime and scalability of a cathode-supported SOFC.

Enlarged plots of CPs vs. $l_a$ and CPs vs. $l_c$ are shown in Figs. 3(b) and 4(b), respectively. Throughout the range of thicknesses from 0 to 1 mm, with the thickness of a cathode sample fixed, CP increases with the increase of *T* as *T* increases from 650 to 800 °C. However, within this range, with the thickness of an anode fixed, CP does not show a monotonic increasing or decreasing dependence on *T*; the CP at 700 °C is the largest among the four temperatures, followed by those at 800, 650 and 700 °C, respectively. Since the thickness of an electrode is generally within the range of 0–1 mm, the enlarged plots in this range enables one to evaluate an electrode thickness once a working temperature is chosen [16,18].

## 5. Conclusion

In summary, quantitative analysis shows the efficiency of effective binary diffusivity measurements on porous anodes or cathodes is doubled by using a bi-sensor electrochemical cell with an oxygen pump across two YSZ tubes. The design provides the opportunity to directly and effectively measure the binary diffusivities of two anodes or two cathodes in an out-of-cell fashion without switching the electrodes out of the furnace between measurements. The facile measurement using the design allows one to do thickness dependent study on CPs, as well as the temperature and current density dependent evaluations. The temperature-dependence of concentration polarization varies as a function of the thickness of anodes and cathodes. The critical thicknesses, above which CPs go straight up, as well as the crossing features of CP vs. *l* curves for different temperatures enable one to design and fabricate low-CP and long-lifetime SOFCs with pre-evaluated electrode thicknesses at working conditions.

## Acknowledgements

The authors are grateful to Professor Srikanth Gopalan at Boston University, Dr. Kyung Joong Yoon at Pacific Northwest National Laboratory and Professor John Goodenough at University of Texas at Austin for their insightful discussions.

## References

[1] M.J. Zhi, N. Mariani, R. Gemmen, K. Gerdes, N.Q. Wu, Energy Environ. Sci. 4 (2) (2011) 417–420.
[2] M.J. Zhi, G.W. Zhou, Z.L. Hong, J. Wang, R. Gemmen, K. Gerdes, A. Manivannan, D.L. Ma, N.Q. Wu, Energy Environ. Sci. 4 (1) (2011) 139–144.
[3] C.S. Ding, T. Hashida, Energy Environ. Sci. 3 (11) (2010) 1729–1731.
[4] S.H. Chan, K.A. Khor, Z.T. Xia, J. Power Sources 93 (1–2) (2001) 130–140.
[5] H. Yakabe, M. Hishinuma, M. Uratani, Y. Matsuzaki, I. Yasuda, J. Power Sources 86 (1–2) (2000) 423–431.
[6] D. Parfitt, A. Chroneos, A. Tarancon, J.A. Kilner, J. Mater. Chem. 21 (7) (2011) 2183–2186.
[7] Y.X. Shi, N.S. Cai, C. Li, J. Power Sources 164 (2) (2007) 639–648.
[8] J.R. Wilson, W. Kobsiriphat, R. Mendoza, H.Y. Chen, J.M. Hiller, D.J. Miller, K. Thornton, P.W. Voorhees, S.B. Adler, S.A. Barnett, Nat. Mater. 5 (7) (2006) 541–544.
[9] K. Huang, J.L. Shull, J. Electrochem. Soc. 158 (2) (2011) B84–B90.
[10] K. Eguchi, Y. Kunisa, K. Adachi, H. Arai, J. Electrochem. Soc. 143 (11) (1996) 3699–3703.
[11] E.J. Crumlin, E. Mutoro, S.J. Ahn, G.J. la O', D.N. Leonard, A. Borisevich, M.D. Biegalski, H.M. Christen, Y. Shao-Horn, J. Phys. Chem. Lett. 1 (21) (2010) 3149–3155.
[12] Y. Patcharavorachot, A. Arpornwichanop, A. Chuachuensuk, J. Power Sources 177 (2) (2008) 254–261.
[13] K.J. Yoon, P. Zink, S. Gopalan, U.B. Pal, J. Power Sources 172 (1) (2007) 39–49.
[14] S.H. Chan, H.K. Ho, Y. Tian, J. Power Sources 109 (1) (2002) 111–120.
[15] Y. Jiang, A.V. Virkar, J. Electrochem. Soc. 150 (7) (2003) A942–A951.
[16] W.D. He, K.J. Yoon, R.S. Eriksen, S. Gopalan, S.N. Basu, U.B. Pal, J. Power Sources 195 (2) (2010) 532–535.
[17] J.W. Kim, A.V. Virkar, K.Z. Fung, K. Mehta, S.C. Singhal, J. Electrochem. Soc. 146 (1) (1999) 69–78.
[18] F. Zhao, T.J. Armstrong, A.V. Virkar, J. Electrochem. Soc. 150 (3) (2003) A249–A256.
[19] K.J. Yoon, S. Gopalan, U.B. Pal, J. Electrochem. Soc. 156 (3) (2009) B311–B317.
[20] F. Zhao, A.V. Virkar, J. Power Sources 141 (1) (2005) 79–95.
[21] A.S. Arico, P. Bruce, B. Scrosati, J.M. Tarascon, W. Van Schalkwijk, Nat. Mater. 4 (5) (2005) 366–377.
[22] T.Z. Sholklapper, H. Kurokawa, C.P. Jacobson, S.J. Visco, L.C. De Jonghe, Nano Lett. 7 (7) (2007) 2136–2141.
[23] P.C. Su, C.C. Chao, J.H. Shim, R. Fasching, F.B. Prinz, Nano Lett. 8 (8) (2008) 2289–2292.
[24] F. Zhao, Z.Y. Wang, M.F. Liu, L. Zhang, C.R. Xia, F.L. Chen, J. Power Sources 185 (1) (2008) 13–18.
[25] E. Fabbri, A. D'Epifanio, S. Sanna, E. Di Bartolomeo, G. Balestrino, S. Licoccia, E. Traversa, Energy Environ. Sci. 3 (5) (2010) 618–621.